Acta Mech 230, 3825–3838 (2019)
https://doi.org/10.1007/s00707-019-02377-z

ORIGINAL PAPER

Milan Batista

Elastic belt extended by two equal rigid pulleys

Received: 22 October 2018 / Revised: 7 January 2019 / Published online: 11 March 2019

Abstract In this paper, we provide an analytical solution for the contact problem of an elastic belt extended by two equal smooth rigid pulleys. The belt is treated as a Bernoulli–Euler rod, and the expressions for pulley displacement and pulley reaction force are given in terms of Jacobi elliptical functions. Theoretical considerations are enhanced by examples in tabular and graphical form.

1 Introduction

This report was motivated by the recent works of Belyaev et al. [1–3]. In these articles, the authors considered an elastic belt stretched by a pair of equal smooth, rigid pulleys. In particular, they considered the belt as a Cosserat flexible rod [3], a Cosserat extensible rod [1], and a Cosserat extensible and shearable rod [2]. From general theory, they derived a set of first-order differential equations and formulated a boundary value problem for which a numerical solution was obtained. Based on this approach, they obtained the deformed shape of the belt, the internal reactions forces and moment, and the contact pressure between the belt and the pulley. The authors devoted particular interest to the transition from the contact area to the belt free span. They found that for a flexible and an extensible belt at the endpoint of the contact a concentrated reaction occurs but for a shearable belt, the transition is smooth. More on contact problems of elastic rods and rigid surfaces, see [4–8] and references there.

In this investigation, a flexible elastic belt [3] will be considered once again. The aim is to develop an analytical solution to the problem. Here analytical solution means that instead of the numerical solution of the governing differential equations we use their closed-form analytical solution and thus reduce the problem to the solution of a system of two transcendental equations. Here analytical means that, in particular, it will be shown that the point contact considered in [3], in which there is a gap between the belt and the pulley, is not possible.

2 Governing equations

We treat the equilibrium condition of a belt of radius a set on two equal smooth rigid pulleys of radius $b < a$ (Fig 1). It is assumed that the lower pulley is fixed and the upper is movable upward. We further stipulate that the belt is weightless, inextensible and unshearable. Thus, the belt may be considered as a plane Bernoulli–Euler rod [9,10]. In addition, we may discuss only a quarter of the belt because of the geometric symmetry of the problem. In what follows, we thus consider a rod of length $\ell = \pi a/2$ with a constant flexural rigidity *EI*.

M. Batista (✉)
Faculty of Maritime Studies and Transport, University of Ljubljana, Ljubljana, Slovenia
E-mail: milan.batista@fpp.uni-lj.si

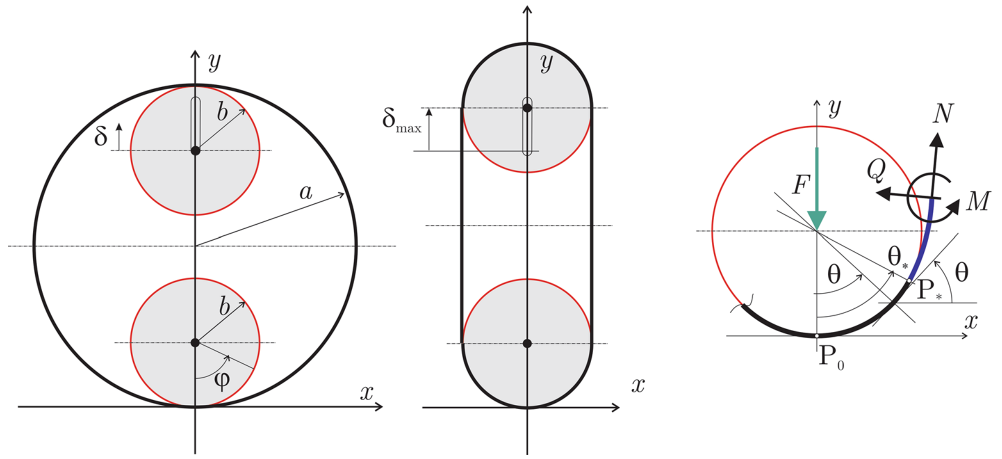

Fig. 1 Initial configuration (left), final configuration (center), and the geometry of the contact (right)

The geometry of the rod is described by the following well-known equations:

$$\frac{\mathrm{d}x}{\mathrm{d}s}=\cos\theta,\quad \frac{\mathrm{d}y}{\mathrm{d}s}=\sin\theta,\quad \frac{\mathrm{d}\theta}{\mathrm{d}s}=\kappa \tag{1.1–3}$$

where $0\le s\le \ell$ is the arc-length, $x(s)$ and $y(s)$ are the coordinates of the rod base curve, $\theta(s)$ is the tangent angle and $\kappa(s)$ is the curvature. The equilibrium equations are [9]:

$$\frac{\mathrm{d}N}{\mathrm{d}s}-\kappa Q+n=0,\quad \frac{\mathrm{d}Q}{\mathrm{d}s}+\kappa N+q=0,\quad \frac{\mathrm{d}M}{\mathrm{d}s}+Q=0 \tag{2.1–3}$$

where $N(s)$, $Q(s)$, and $M(s)$ are the internal normal force, shear force, and bending moment acting over the cross section of the rod, and $n(s)$ and $q(s)$ are the load intensity in the directions of $N$and Q, respectively. For the following discussion related to the rod, the constitutive equation connects the moment with the curvature. There are two possibilities [11]:

$$M=\mathrm{EI}\left(\kappa-\frac{1}{a}\right); \tag{3.1}$$

$$M=\mathrm{EI}\kappa. \tag{3.2}$$

In the case (3.1), the initial state of the belt is stressless, while in the case (3.2) the belt is bent into a circle with the bending moment $M=\mathrm{EI}/a$. In what follows, we will for M use (3.1), unless otherwise stated.

When the upper pulley is displaced by δ, the belt is stretched, and there is a reaction force F on each pulley. For $0\le\delta\le\delta_0$, where δ_0 is some limiting value of the displacement which depends on b, the belt touches the pulley at the apex point P_0. For $\delta_0<\delta\le\delta_{\max}$ the belt is in contact with the pulley from P_0 to the endpoint P_*. We assume that this contact is conformal, i.e., full line contact. Therefore, the maximal displacement $\delta_{\max}$ is:

$$\delta_{\max}=(\pi-2)(a-b). \tag{4}$$

In any case, the rod has two parts: the part that is in contact with the pulley and the portion which is unsupported. We can thus divide the length of the rod ℓ as:

$$\ell=\ell_c+\ell_f \tag{5}$$

where $0\le\ell_c\le\pi b/2$ is the length of the contact, and $\pi(a-b)/2\le\ell_f\le\pi a/2$ is the length of the free span.

In what follows, Eqs. (1), (2), and (3) will be separately considered for the contact and the free span cases. We will assume that the coordinates x, y, and the angle θ are continuous and differentiable functions of s, at P_*. Also, we will suppose that at this point the normal force $N$and bending moment M are continuous because of the absence of a concentrated reaction tension and moment [1–3]. However, the shear force Q has a jump at P_* as shown in [1,3].

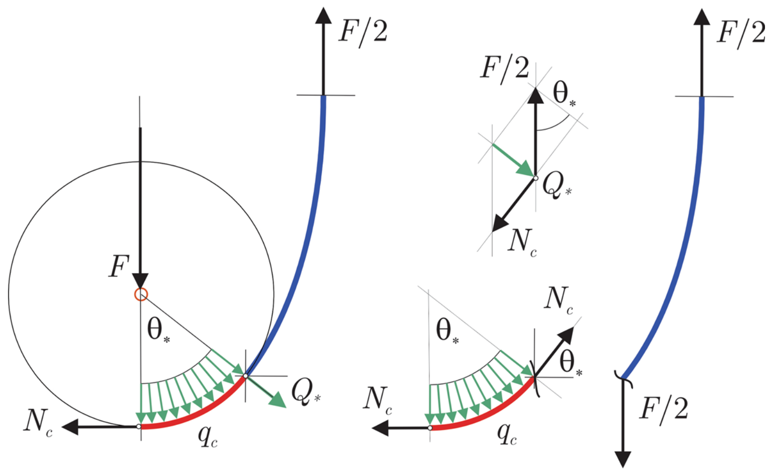

Fig. 2 Equilibrium of forces acting on a quarter of the ring

3 The contact

The shape of the rod which is in contact with the lower pulley is given by:

$$x = b \sin \varphi, \quad y = b\,(1 - \cos \varphi)\,, \tag{6}$$

where φ is the central angle. By differentiating (6) with respect to φ and then comparing the results with (1), we find that:

$$\varphi = \theta, \quad \kappa = \frac{1}{b}, \quad s = b\theta, \tag{7}$$

while the length of contact is:

$$\ell_c = b \int_0^{\theta_*} \mathrm{d}\theta = b\theta_*. \tag{8}$$

Because $\kappa = \text{const}$, M, and therefore the equilibrium equations (2) reduce to:

$$\frac{\mathrm{d}N}{\mathrm{d}s} + n = 0, \quad q = -\frac{N}{b}, \quad Q = 0. \tag{9}$$

The problem is thus indeterminate unless we make some assumptions regarding n, which in our case is related to the friction intensity between the ring and the pulley. We assumed smooth pulleys, so we can set the following:

$$n\,(s) = 0, \tag{10}$$

and so, from (9), $N = N_c = \text{const}$. The part of the belt in contact with the pulley is thus subject to the constant bending moment M_c and reaction intensity q_c which are given by:

$$M_c = \mathrm{EI}\left(\frac{1}{b} - \frac{1}{a}\right), \quad q_c = \frac{N_c}{b}, \tag{11.1,2}$$

and the constant internal tension N_c, while the shear force Q vanishes.

To obtain N_c, we consider the equilibrium of the forces acting on the rod (Fig. 2). As previously indicated, the supported part of the belt is subject to the internal tension N_c, while the free part is subject to the constant internal force $F/2$, by assuming that the normal force is continuous. Consequently, the concentrated shear reaction force Q_* must arise at the end of the contact to maintain the overall equilibrium of the rod. We obtain the expressions for N_c and Q_* by considering the equilibrium of the forces in the horizontal and vertical directions. We therefore have:

$$-N_c + Q_* \sin\theta_* + b\int_0^{\theta_*} q_c \sin\theta d\theta = 0, \tag{12}$$

$$\frac{F}{2} - Q_* \cos\theta_* - b\int_0^{\theta_*} q_c \cos\theta d\theta = 0, \tag{13}$$

where θ_* is the contact angle. After integration and using (11.2) for q_c, we obtain the following system of equations:

$$Q_* \sin\theta_* - N_c \cos\theta_* = 0, \quad Q_* \cos\theta_* + N_c \sin\theta_* = \frac{F}{2}. \tag{14}$$

The solution for N_c and Q_* is therefore:

$$N_c = \frac{F}{2}\sin\theta_*, \tag{15}$$

$$Q_* = \frac{F}{2}\cos\theta_*. \tag{16}$$

We summarize the results obtained in this Section as follows. The contact between the belt and the pulleys is entirely determinate once the contact angle θ_* and the reaction force F are known. In this case , we can calculate the contact length ℓ_c from (8), internal tension force N_c by (15), shear reaction force Q_* by (16), and the internal bending moment M_c and contact intensity q_c by (11). For the point contact when $\theta_* = 0$, we have:

$$\ell_c = 0, \quad N_c = 0, \quad Q_* = \frac{F}{2}, \quad q = 0, \tag{17}$$

while the bending moment M_c depends on the curvature of the rod at the apex.

The results presented in this Section were obtained by Belyaev and coauthors [3] in a slightly different way.

4 The free span

For the free span, we have $n = q = 0$, so this part of the rod is subject only to a constant terminal force $F/2$. For such a rod, the general solution for Eqs. (1), (2), and (3) is given in the "Appendix". In our case, the force inclination angle α and the rod initial coordinates x_0, y_0 are:

$$\alpha = \frac{\pi}{2}, \quad x_0 = b\sin\theta_*, \quad y_0 = b\left(1-\cos\theta_*\right). \tag{18}$$

Using the expressions found in (47), (50), (51), (52), (53), we obtain the internal forces:

$$N = \frac{F}{2}\sin\theta, \quad Q = \frac{F}{2}\cos\theta, \tag{19}$$

the tangent angle

$$\theta = -\frac{\pi}{2} + 2\mathrm{am}\left(k\omega\sigma + C, k^{-1}\right), \tag{20}$$

the curvature

$$\kappa = 2\ell_f^{-1}\omega k \mathrm{dn}\left(k\omega\sigma + C, k^{-1}\right), \tag{21}$$

and the coordinates

$$x = b\sin\theta_* + \ell_f \frac{2k}{\omega}\left[\mathrm{dn}\left(C, k^{-1}\right) - \mathrm{dn}\left(k\omega\sigma + C, k^{-1}\right)\right], \tag{22}$$

$$y = b\left(1-\cos\theta_*\right) + \ell_f\left[\left(2k^2-1\right)\sigma + \frac{2k}{\omega}\left[\varepsilon\left(C, k^{-1}\right) - \varepsilon\left(k\omega\sigma + C, k^{-1}\right)\right]\right], \tag{23}$$

where $0 \leq \sigma \equiv \frac{s}{\ell_f} \leq 1$ and ω is the load parameter (49) defined as:

$$\omega^2 \equiv \frac{F\ell_f^2}{2EI}. \tag{24}$$

The length of the free span ℓ_f using (8) for ℓ_c is given as:

$$\ell_f = \ell - \ell_c = \frac{\pi a}{2} - b\theta_*. \tag{25}$$

The values of k, C, and θ_* depend on the boundary conditions. In our case, these conditions are, by treating θ and κ as functions of σ:

$$\theta\,(0) = \theta_*, \quad \theta\,(1) = \frac{\pi}{2}, \tag{26}$$

and when $\theta_* > 0$, we assume:

$$\kappa\,(0) = \frac{1}{b}. \tag{27}$$

This last equation requires that at the endpoint P_* the belt and the pulley have contact of order two, i.e., the same tangent and the same curvature. For the Bernoulli–Euler rod, this also means that at P_*, the bending moment is continuous.

Introducing the boundary conditions (26) into the expression (20) for θ and solving for C and ω, we obtain:

$$C = \mathrm{am}^{-1}\left(\frac{\pi}{4} + \frac{\theta_*}{2}, k^{-1}\right), \tag{28}$$

$$\omega = k^{-1}\left[K\left(k^{-1}\right) - \mathrm{am}^{-1}\left(\frac{\pi}{4} + \frac{\theta_*}{2}, k^{-1}\right)\right]. \tag{29}$$

Introducing boundary condition (27) into expression (21) for κ, we obtain $\kappa\,(0) = 2\ell_f^{-1}\omega k \mathrm{dn}\left(C, k^{-1}\right) = 1/b$ or, using (28) for C and (25) for ℓ_f, we have:

$$\frac{b}{a} = \frac{\pi}{2\left(\theta_* + \sqrt{2}\omega\sqrt{2k^2 - 1 - \sin\theta_*}\right)}. \tag{30}$$

With expression (29) for ω, we can calculate the reaction force F using (24). However, instead of force F,we calculate the dimensionless load factor which we define as follows:

$$\frac{Fa^2}{\mathrm{EI}} = \frac{2a^2\omega^2}{\ell_f^2} = \frac{2}{k^2}\left[\frac{K\left(k^{-1}\right) - C}{\pi - 2b\theta_*/a}\right]^2. \tag{31}$$

When k, θ_* are known then we can calculate ω,C by (28), (29), and further we can calculate the coordinates x and y of the rod using (22) and (23). In particular, the displacement δ is given by $\delta = 2\,[y\,(1) - a]$ or in explicit form

$$\frac{\delta}{a} = 2\left[\frac{b}{a}\,(1 - \cos\theta_*) - 1\right] + 2\left(\frac{\pi}{2} - \frac{b}{a}\theta_*\right)\left\{2k^2\left[1 - \frac{E\left(k^{-1}\right) - \varepsilon\left(C, k^{-1}\right)}{K\left(k^{-1}\right) - C}\right] - 1\right\}. \tag{32}$$

At our disposal, we now have expressions (30), (31), (32) that contain five parameters: k, θ_*, b, F, and δ. Two must be given, and the other three can then be calculated. However, only the case when b and either F or δ are given, and k and θ_* are to be calculated is of practical interest. In either case when $\theta_* > 0$, we must solve a system of two nonlinear Eqs. (30) and (31), or (30) and (32).

The point contact when $\theta_* = 0$ reduces the expressions (31) and (32) to:

Table 1 Results for the calculation for $b/a = 0.5$ when $Fa^2/\mathrm{EI} = 5$ (case 1, Fig. 4) and when $\delta/a = 0.5$ (case 2, Fig. 5)

Case	δ/a	Fa^2/EI	N_c/F	Q_*/F	qa/F	ℓ_c/a	ω
1	0.217525	5	0.239154	0.485491	0.239154	0.120747	2.29273
2	0.5	8.25294	0.26333	0.42504	0.52665	0.277329	2.62751

$$\frac{Fa^2}{\mathrm{EI}} = \frac{8}{\pi^2 k^2}\left[K\left(k^{-1}\right) - \mathrm{am}^{-1}\left(\pi/4, k^{-1}\right)\right]^2, \tag{33}$$

$$\frac{\delta}{a} = \pi\left\{2k^2\left[1 - \frac{E\left(k^{-1}\right) - \varepsilon\left(\mathrm{am}^{-1}\left(\pi/4, k^{-1}\right), k^{-1}\right)}{K\left(k^{-1}\right) - \mathrm{am}^{-1}\left(\pi/4, k^{-1}\right)}\right] - 1\right\} - 2, \tag{34}$$

while formula (30) becomes:

$$\frac{b}{a} = \frac{\pi\sqrt{2}}{4\left[K\left(k^{-1}\right) - \mathrm{am}^{-1}\left(\frac{\pi}{4}, k^{-1}\right)\right]\sqrt{2-k^{-2}}}. \tag{35}$$

If b is given, then we can calculate the limiting value of k_0 from (35) for which the belt begins to come into contact with the pulley. Thus, for $k_0 \le k < \infty$, we have a point contact, while for $1 < k < k_0$, we have a line contact. Once k_0 is known, we can calculate the limiting force F_0 and the limiting displacement δ_0 by (33) and (34).

We can summarize the results of this Section in the following algorithms:

given: b, F	given: b, δ
solve (35) for k_0	solve (35) for k_0
calculate $F_0$by(33)	calculate $\delta_0$by(34)
if $F < F_0$	**if** $\delta < \delta_0$
solve (33) for k	solve (34) for k
else	**else**
solve (30) and (31) for k and θ_*	solve (30) and (32) for k and θ_*
end	**end**

Once k and θ_* are obtained, all the other quantities can be calculated from (19)–(23).

5 Examples

For practical calculations, we used the Elfun18 library [12]. This library implements the double-precision numerical model and thus can calculate $K\left(k^{-1}\right)$ only for $k \ge 1 + 0.5 \times 10^{-15}$. For the smallest k and $\theta_* = 0$, we have $b/a \approx 0.0504843$, $\omega \approx 17.833600$, $\frac{Fa^2}{\mathrm{EI}} \approx 257.791325$, $\frac{\delta}{a} \approx 0.5191998$, and $\frac{\delta_{\max}}{a} \approx 0.541980$. For values of k that are close to one, we used a Maple program for the calculation with the quad-precision numerical model.

As seen in the previous Section, the solution to the problem can be reduced to the solution of a nonlinear equation or a system of two nonlinear equations. Now, Eq. (35) is easily solved numerically for k by the false position method for example, because b, given by (35), is a monotone function of k (Fig. 3). To accomplish this, in (35) we replace $k' = k^{-1}$ and then seek a solution in the interval $k' \in [0, 1)$. Similarly, we can solve Eqs. (33) and (34) for k. Inspection of the graphs shown in Figs. 4 and 5 indicates that the systems have a unique solution for $k' \in [0, 1)$ and $\theta_* \in [0, \pi/2)$.

Given the present solution, we can also easily construct various diagrams (Figs. 6, 7, and 8). From the graphs shown in Fig. 6, where the dependence of the limiting displacement δ_0 on b/a is represented, we can see that when $b/a \le 0.5$ the belt is in point contact with the pulley for most of the displacement δ. As can be seen from the graphs shown in Figs. 7 and 8 where the dependence of the load factor Fa^2/EI and the contact angle θ_* on the displacement δ are shown, the belt becomes stiff once the line contact is reached. Moreover, $Fa^2/\mathrm{EI} \to \infty$ and $\theta_* \to \pi/2$ as $\delta \to \delta_{\max}$.

For verification of the present solution, we consider three cases. The first is a ring in tension [11,13]. In this case, $b = 0$ and therefore $\theta_* = 0$. Therefore, we have to solve Eq. (33) for unknown k when F is given.

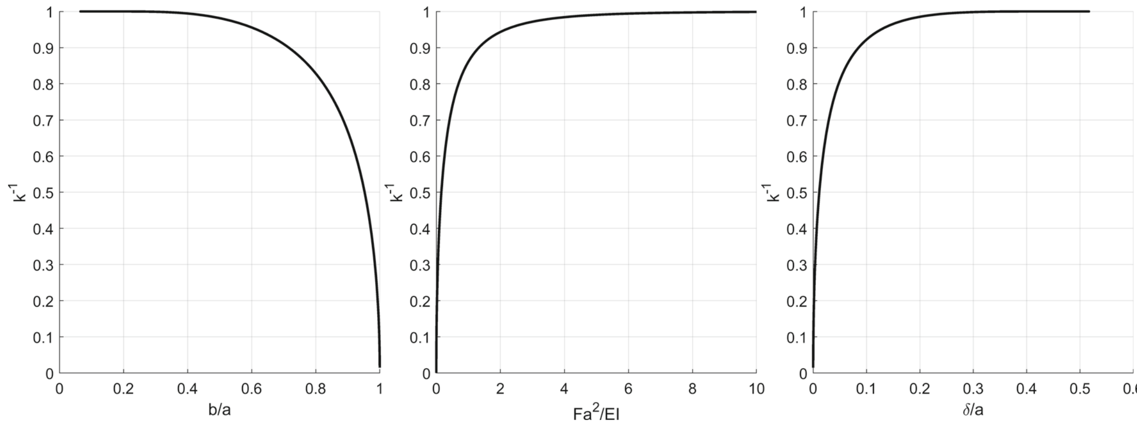

Fig. 3 The inverse of the elliptic modulus k^{-1} as a function of the pulley radius b/a, the load factor Fa^2/EI, and the displacement δ/a when $\theta_* = 0$

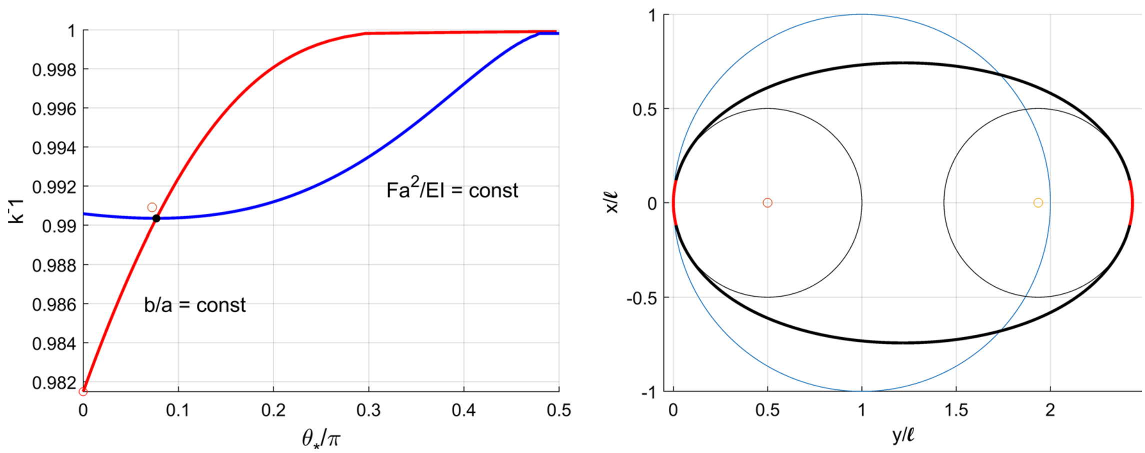

Fig. 4 The intersection of (30) and (31) when $b/a = 0.5$ and $Fa^2/\mathrm{EI} = 5$. The intersection point is at $k \approx 1.0097410$ and $\theta_* \approx 0.2414942$. Empty point near intersection is an initial guess. Corresponding belt shape (right)

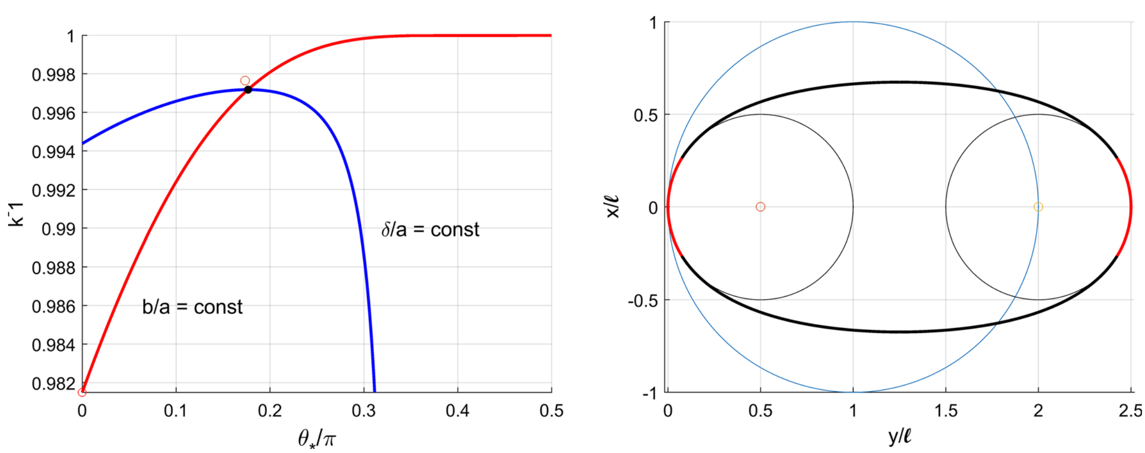

Fig. 5 The intersection of (30) and (32) when $b/a = 0.5$ and $\delta/a = 0.5$; $k \approx 1.0028281$, $\theta_* \approx 0.5546579$. Empty point near intersection is an initial guess (left). Corresponding belt shape (right)

The results presented in Table 2 are in good agreement with those of Frisch-Fay [11] (Table 3 on page 122 therein).

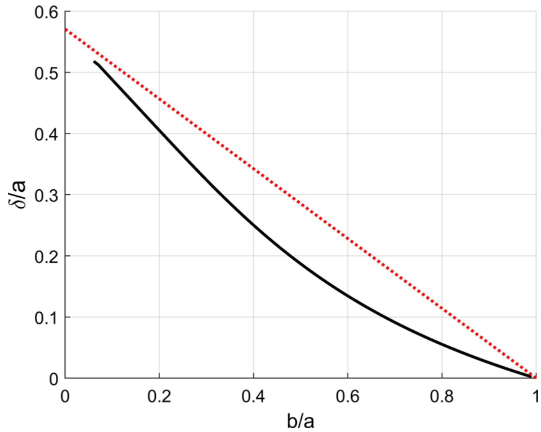

Fig. 6 Limiting displacement δ_0 (solid line) and maximal displacement $\delta_{\max}$ (dotted line) as a function of pulley radius b/a. The maximum difference between displacements $(\delta_{\max} - \delta_0)/a \approx 0.098423$ occurs at $b/a \approx 0.505249$

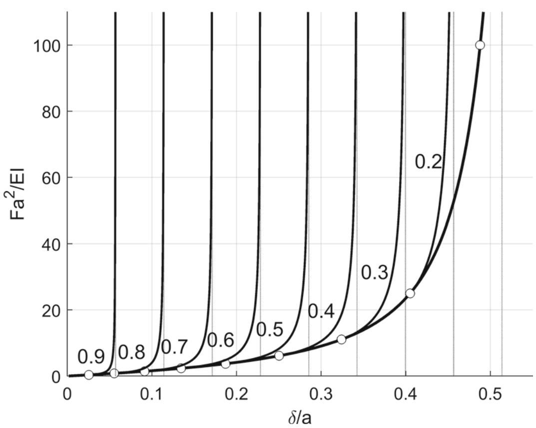

Fig. 7 Load factor Fa^2/EI as a function of the dimensionless displacement δ/a for various values of the dimensionless pulley radius b/a. Dots indicate the beginning of the line contact. Dotted vertical lines indicate the maximum displacement for corresponding b/a. (ex1a)

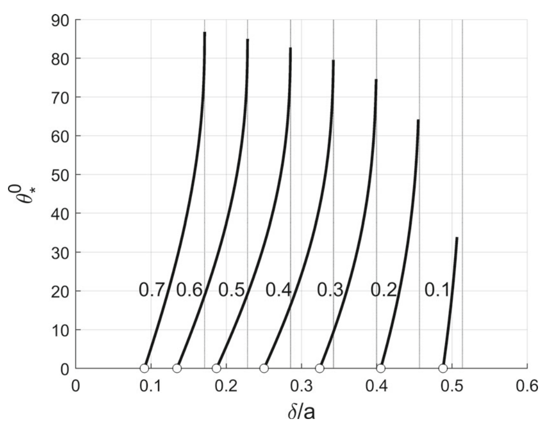

Fig. 8 Contact angle θ_* as a function of dimensionless displacement δ/a for various values of dimensionless pulley radius b/a. The dots indicate the beginning of the line contact. Dotted vertical lines indicate the maximum displacement for corresponding b/a. (ex2)

The second example is from [2] where the authors consider extensible and shearable rods. However, we consider only a flexular rod where the belt and the pulley radii are 0.25 m and 0.1 m, respectively, Young's modulus is 1 GPa, and the cross section of the rod is a square with a side of 0.01 m. The pulleys are separated

Table 2 Ring in tension: $a = 10$, $\mathrm{EI} = 20$. The calculated moments do not include the initial curvature

$F/2$			0.0313				1.682	
	M (1)	M (0)	x (1)	y (1)	M (1)	M (0)	x (1)	y (1)
[11]	− 1.884	− 2.191	9.782	10.2231	− 0.202	− 8.205	4.758	13.6848
Present*	1.8899	2.1963	9.7889	10.2246	0.2020	8.2049	4.7580	13.6923

Table 3 Comparison of calculations; $a = 0.25$ m, $b = 0.1$ m, $EI = 0.8\dot{3}\ \mathrm{Nm}^2$, $F = 200$ N

	θ_* (rad)	ℓ_c (m)	δ (m)	N_c (N)	Q_* (N)	q(N/m)	M_c (Nm)
Numeric [2]*	0.678	0.068	0.159	$\sim$ 58.5	$\sim$ 79	–	$\sim$ 5
Present	0.62448	0.06245	0.15851	58.4674	81.1268	584.674	5

*Shearable and extensible rod. Values for N, Q, and M are estimated from Figs. 5 and 6 therein

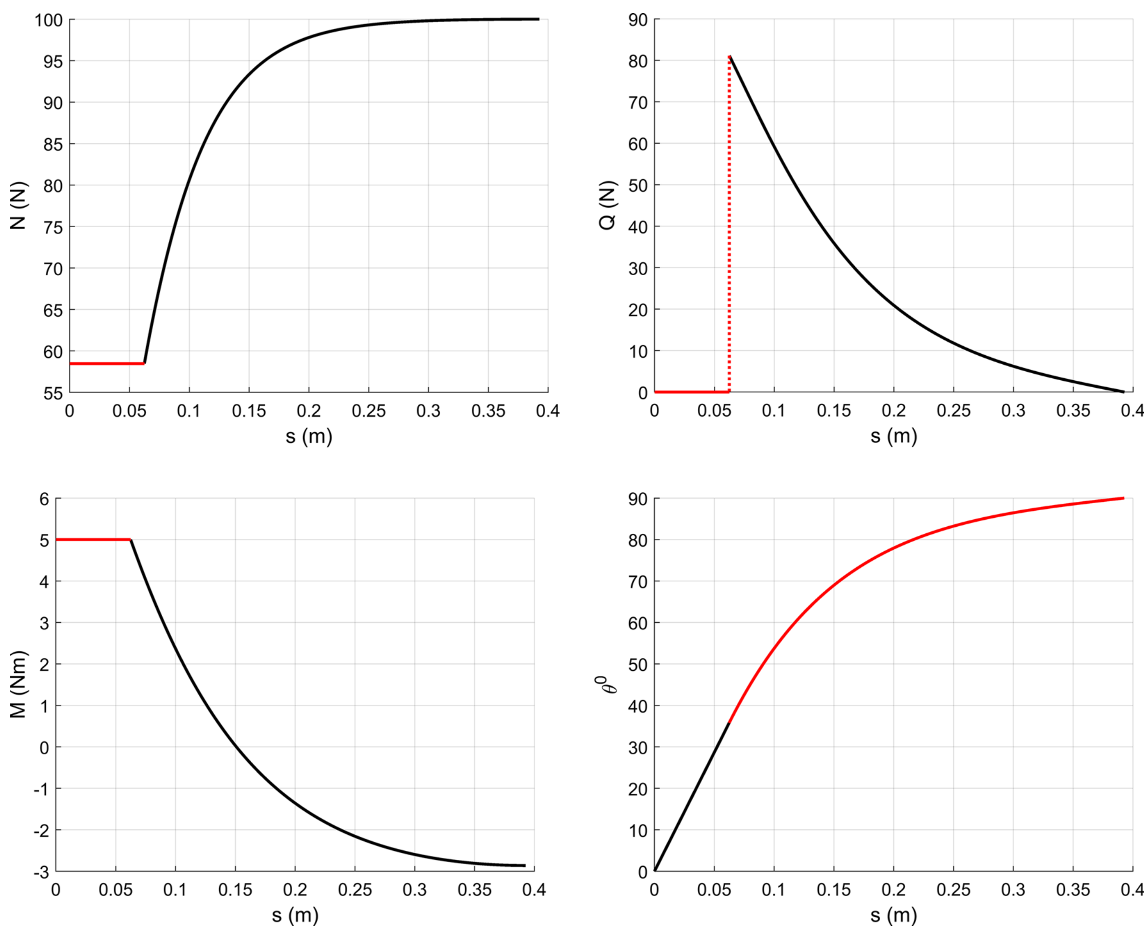

Fig. 9 Normal force N, shear force Q, bending moment M, and tangent angle θ as a function of material coordinate s for the data in Table 3

by a force of 200 N. The solution of Eqs. (30) and (31) for these data is $k \approx 1.00034$ and $\theta_* \approx 0.624479$. The results of the calculation are given in Table 3, and Figs. 9 and 10. A comparison of the distribution of internal forces and the moment along the rod is displayed in Fig. 9, where the graphs in Figs. 5 and 6 in [2] indicate that the shear properties of the belt influence only narrow neighbors of the endpoint of the contact.

The last example is from [3]. The ring and the pulley radius are 0.55 m and 0.15 m, respectively. Young's modulus is 0.1 GPa, and the cross section is a square with a side of 0.01 m. The pulley displacement is 0.228 m, which is very close to the maximum of $\sim$ 0.2283185m. In this case, k is very close to one, so for the solution

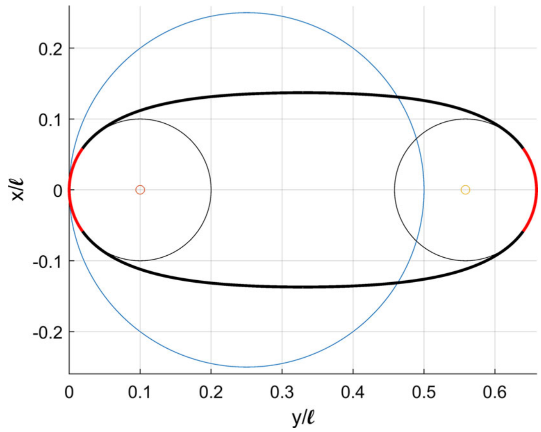

Fig. 10 Belt and pulleys for the case from Table 3

Table 4 Comparison of calculation; $a = 0.55$ m, $b = 0.15$ m, $\mathrm{EI} = 0.08\dot{3}$ Nm^2, $\delta = 0.228$ m

	θ_* (rad)	ℓ_f (m)	F (N)	Q_* (N)	q(N/m)
Numeric [3]	1.28	0.672	87.6	12.5	280
Present	1.275776	0.672572	85.726670	12.4628941	273.409889
Difference %	0.33	0.08	1.02	0.30	2.41

of the equations, we use a Maple program with the number of digits set to 32. The solutions of Eqs. (30) and (32) are:

$$\begin{aligned} k &= 1.0000000000000002461214898165095 \\ \theta_* &= 1.2757764592145434757876907155969 \end{aligned}, \tag{36}$$

and from this

$$\begin{aligned} C &= 2.6051913681753288856298889866486 \\ \omega &= 15.253590055581034632534643842961 \end{aligned}. \tag{37}$$

The absolute error of the solution is 4.3×10^{-23}. As seen from Table 4, the relative discrepancy of the results obtained in [3] by the numerical method and present analytical is within 2.5%.

Point contact

In [3] the authors numerically test the hypothesis that once the force F or displacement δ is higher than the limiting value F_0 or δ_0, the reaction force Q_* splits the rod into two parts in such a way that there is a gap between the pulley and the rod between, i.e., between the apex point P_0 and the contact point P_* (Fig. 11). Therefore, the lower part of the rod has the shape of the elastic curve similar to the upper one. In order to determine whether this curve intersects the pulley circle, it is sufficient to consider only the lower part of the rod. The quantities that belong to this part of the rod will be in the sequel denoted by subscript 1.

The lower part is subject to the terminal load Q_* that has the inclination angle given by:

$$\alpha_1 = -\frac{\pi}{2} - \theta_*. \tag{38}$$

Using the solution given in "Appendix" we set $\sigma = \frac{s}{\ell_1}$, where ℓ_1 is the part length. The boundary conditions are:

$$\theta_1(0) = 0, \quad \theta_1(1) = \theta_*. \tag{39}$$

Introducing these into (50) we get:

$$C_1 = -\mathrm{am}^{-1}\left(\frac{\pi}{4} + \frac{\theta_*}{2}, k_1^{-1}\right), \quad \omega_1 = k_1^{-1}\left[\mathrm{am}^{-1}\left(\frac{\pi}{4} + \frac{\theta_*}{2}, k_1^{-1}\right) - \mathrm{am}^{-1}\left(\frac{\pi}{4}, k_1^{-1}\right)\right]. \tag{40}$$

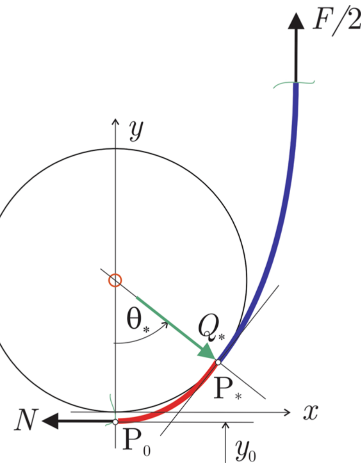

Fig. 11 Assumed shape of the rod for the point contact

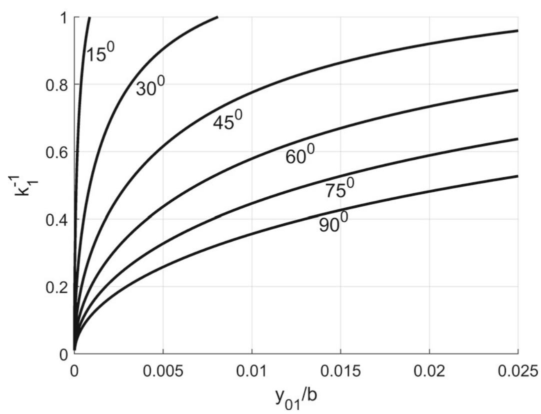

Fig. 12 The nondimensional vertical position of the apex y_0/b of the rod as a function of the inverse of the elliptic modulus k^{-1} for various values of contact angles θ_*

To obtain ℓ_1 and the coordinates x_{01} and y_{01} of P_0, we need three equations. Because$x_1(0) = 0$, we have $x_{01} = 0$. Next, the contact with the pulley requires

$$x_1(1) = b\sin\theta_*, \quad y_1(1) = b(1-\cos\theta_*) \quad . \tag{41}$$

By substituting these into (52), (53), we find:

$$\ell_1 = -b\frac{\sin\theta_*}{\hat{\xi}_1\sin\theta_* + \hat{\eta}_1\cos\theta_*}, \tag{42}$$

$$y_{01} = b(1-\cos\theta_*) + \ell_1\left(-\hat{\xi}_1\cos\theta_* + \hat{\eta}_1\sin\theta_*\right) \tag{43}$$

where

$$\hat{\xi}_1 = \frac{2k_1}{\omega_1}\left[\varepsilon\left(k_1\omega_1 + C_1, k_1^{-1}\right) - \varepsilon\left(C_1, k_1^{-1}\right)\right] - \left(2k_1^2 - 1\right), \tag{44}$$

$$\hat{\eta}_1 = \frac{2k_1}{\omega_1}\left[\mathrm{dn}\left(C_1, k_1^{-1}\right) - \mathrm{dn}\left(k_1\omega_1 + C_1, k_1^{-1}\right)\right]. \tag{45}$$

Now, if $y_{01} < 0$ then there is a gap between the rod and the pulley, and if $y_0 > 0$, then the curve intersects the pulley circle. For small $\theta_* > 0$ the expansion of (43) in a power series gives:

$$\frac{y_{01}}{b} = \frac{\theta_*^3}{24\left(2k^2-1\right)}\left[1 + \frac{\theta_*}{2\left(2k^2-1\right)} + \cdots\right] > 0. \tag{46}$$

For larger θ_*, the situation is presented graphically in Fig. 12 where the graph of y_{01} given by (43) is shown for various values of θ_*. The characteristic of these graphs is that $y_{01} > 0$ for $0 < k_1^{-1} < 1$ and $0 < \theta_* < \pi/2$. On the basis of these results, we conclude that the rod intersects the pulley circle. This conclusion means that the starting assumption of point contact is invalid; once the load is higher than some limiting value, we obtain full line contact between the belt and the pulley. A similar result was obtained in [3] using numerical integration. However, the authors did not make a general conclusion.

6 Conclusions

In this report, we analytically solve the contact problem for a belt with pulleys. For actual calculations, instead of solving the boundary value problem for a set of differential equations, it is necessary to solve one or two nonlinear equations. The present results for the calculations are in good agreement with those reported in the literature. We also show that for a force larger than a limiting force F_0, the belt comes into full line contact with the pulley; i.e., a point contact is not possible.

Appendix

In this Appendix, a solution is provided for Eqs. (1), (2), and (3) for the case when the rod is subject to a terminal conservative force (Fig. 13).

We assume that EI is the rod bending stiffness, ℓ is the rod length, and F is the force with an angle of inclination α. Then, the solution of the force equilibrium equations (2.1,2) is given as:

$$N = -F\cos(\alpha + \theta), \quad Q = F\sin(\theta + \alpha). \tag{47}$$

With these solutions and either of the constitutive Eq. (3.1) or (3.2), the moment Eq. (2.3) becomes:

$$\frac{d^2\theta}{d\sigma^2} + \omega^2 \sin(\theta + \alpha) = 0 \tag{48}$$

where $0 \leq \sigma \equiv \frac{s}{\ell} \leq 1$ is the normalized arc-length parameter and ω is the load parameter which is defined by:

$$\omega^2 \equiv \frac{F\ell^2}{\mathrm{EI}}. \tag{49}$$

The problem discussed in this paper assumes that the rod is bent only in one direction. This case is covered by the non-inflectional solution of (48) which is [10,13,14,14–16]:

$$\theta = -\alpha + 2\,\mathrm{am}\left(k\omega\sigma + C, k^{-1}\right). \tag{50}$$

Once we know θ, we can calculate the curvature by (1.3):

$$\kappa = \ell^{-1} 2\omega k\,\mathrm{dn}\left(k\omega\sigma + C, k^{-1}\right), \tag{51}$$

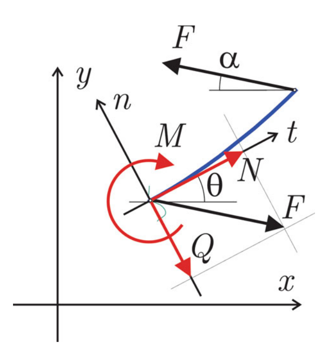

Fig. 13 Equilibrium of the rod segment

and the coordinates by integration of (1.1,2):

$$x = x_0 + \ell \left[\hat{\xi} (\sigma; k, \omega, C, \alpha) \cos\alpha + \hat{\eta} (\sigma; k, \omega, C, \alpha) \sin\alpha \right], \tag{52}$$

$$y = y_0 + \ell \left[-\hat{\xi} (\sigma; k, \omega, C, \alpha) \sin\alpha + \hat{\eta} (\sigma; k, \omega, C, \alpha) \cos\alpha \right] \tag{53}$$

where x_0 and y_0 are some known coordinates of the rod, and

$$\hat{\xi} (\sigma; k, \omega, C) = \frac{2k}{\omega} \left[\varepsilon \left(k\omega\sigma + C, k^{-1} \right) - \varepsilon \left(C, k^{-1} \right) \right] - \left(2k^2 - 1 \right) \sigma, \tag{54}$$

$$\hat{\eta} (\sigma; k, \omega, C) = \frac{2k}{\omega} \left[\mathrm{dn} \left(C, k^{-1} \right) - \mathrm{dn} \left(k\omega\sigma + C, k^{-1} \right) \right]. \tag{55}$$

In the preceding formulas, dn is the Jacobian elliptic function, $\mathrm{am}\,(x, k) \equiv \int_0^x \mathrm{dn}\,(t, k)\, dt$ is the Jacobi's amplitude function, $\varepsilon\,(x, k) \equiv \int_0^x \mathrm{dn}^2\,(t, k)\, dt$ is the Jacobi's epsilon function [17], k is the elliptic modulus, and C is a constant of integration. We note that all the aforementioned elliptical functions are symmetric with respect to k, so we chose:

$$k > 1. \tag{56}$$

Also, because the function am is periodic with a period of $2K$, we can always choose C to lie in the interval

$$-K \le C < K \tag{57}$$

where $K\left(k^{-1}\right)$ is the elliptic integral of the first kind. If we suppose that $\omega \ge 0$ and $k > 1$ then $\kappa > 0$. The solution (50) thus describes the rod that is bent only in one direction as required. The shape of the rod depends on k, C, ω while its location and orientation depend on x_0, y_0, and α.

In an initial state when $\omega = 0$ the solution of Eq. (48) subject to a condition $\theta\,(0) = 0$ is

$$\theta = \frac{s}{a} \tag{58}$$

where $\theta' = 1/a$ is the curvature. In this case, from (1), we obtain, when $x\,(0) = y\,(0) = 0$,

$$x = a \sin\theta, \qquad y = a\,(1 - \cos\theta)\,. \tag{59}$$

Thus, the rod has the shape of a circular arc lying on the circle with radius a. When $a = \infty$ the arc becomes a straight line. We note that from (50) that we obtain a circular arc when $k = \infty$ and a straight line when $k = 0$ [14].

References

1. Belyaev, A., Eliseev, V., Irschik, H., Oborin, E.: Nonlinear statics of extensible elastic belt on two pulleys. PAMM **16**, 11–14 (2016)
2. Belyaev, A.K., Eliseev, V.V., Irschik, H., Oborin, E.A.: Contact of two equal rigid pulleys with a belt modelled as Cosserat nonlinear elastic rod. Acta Mech. **228**, 4425–4434 (2017)
3. Belyaev, A.K., Eliseev, V.V., Irschik, H., Oborin, E.A.: Contact of flexible elastic belt with two pulleys. In: Irschik, H. (ed.) Dynamics and Control of Advanced Structures, pp. 195–203. Springer, Berlin (2017)
4. Denoel, V., Detournay, E.: Eulerian formulation of constrained elastica. Int. J. Solids Struct. **48**, 625–636 (2011)
5. Huynen, A., Detournay, E., Denoel, V.: Eulerian formulation of elastic rods. Proc R. Soc. A Math. Phys. **472**, 1–23 (2016)
6. Huynen, A., Detournay, E., Denoel, V.: Surface constrained elastic rods with application to the sphere. J. Elast. **123**, 203–223 (2016)
7. Majidi, C., O'Reilly, O.M., Williams, J.A.: On the stability of a rod adhering to a rigid surface: shear-induced stable adhesion and the instability of peeling. J. Mech. Phys. Solids **60**, 827–843 (2012)
8. Steinbrecher, I., Humer, A., Vu-Quoc, L.: On the numerical modeling of sliding beams: a comparison of different approaches. J. Sound Vib. **408**, 270–290 (2017)
9. Antman, S.S.: Nonlinear Problems of Elasticity, 2nd edn. Springer, New York (2005)
10. Love, A.E.H.: A Treatise on the Mathematical Theory of Elasticity, 4th edn. Dover Publications, New York (1944)
11. Frisch-Fay, R.: Flexible Bars. Butterworths, London (1962)

12. Batista, M.: Elfun18 A Collection of Matlab functions for the computation of Elliptical Integrals and Jacobian elliptic functions of real arguments. arXiv:1806.10469 [cs.MS] (2018)
13. Popov, E.P.: Theory and Calculation of Flexible Elastic Bars. Nauka, Moscow (1986)
14. Batista, M.: Analytical treatment of equilibrium configurations of cantilever under terminal loads using Jacobi elliptical functions. Int. J. Solids Struct. **51**, 2308–2326 (2014)
15. Batista, M.: A closed-form solution for Reissner planar finite-strain beam using Jacobi elliptic functions. Int. J. Solids Struct. **87**, 153–166 (2016)
16. Goss, V.G.A.: Snap buckling, writhing and loop formation in twisted rods. In: Center for Nonlinear Dynamics, University Collage London, PhD. thesis (2003)
17. Reinhardt, W.P., Walker, P.L.: Jacobian elliptic functions. In: Olver, F.W.J. (ed.) NIST Handbook of Mathematical Functions, p. xv. Cambridge University Press, NIST, Cambridge; New York (2010)